Proceedings of the ASPF 2003 (The 8th Asian Symposium on Precision Forging), October 15 - 18, 2003

PREDICTION OF MICROSTRUCTURE DURING HIGH TEMPERATURE FORMING OF Ti-6Al-4V ALLOY

Y.H. Lee[1], T.J. Shin[2], J.T. Yeom[3], N.K. Park[3], S.S. Hong[4], I.O. Shim[4], S.M. Hwang[2] and C.S. Lee[1]

[1]Dept. of Materials Science and Engineering, POSTECH
[2]Dept. of Mechanical Engineering, POSTECH
San 31 Hyoja-dong, Pohang 790-784, KOREA
[3]Metal Working and Plasticity Group, Dept. of Materials Processing, KIMM
66 Sangnam-dong, Changwon, Kyungnam, 641-010, KOREA
[4]Agency for Defense Development, Daejeon 305-600, KOREA

Abstract

Prediction of final microstructures after high temperature forming of Ti-6Al-4V alloy was attempted in this study. Using two typical microstructures, i.e., equiaxed and Widmanstätten microstructures, compression test was carried out up to the strain level of 0.6 at various temperatures (700 ~ 1100°C) and strain rates (10^{-4} ~ 10^{2}/s). From the flow stress–strain data, parameters such as strain rate sensitivity (m) and activation energy (Q) were calculated and used to establish constitutive equations for both microstructures. Then, finite element analysis was performed to predict the final microstructure of the deformed body, which was well accorded with the experimental results.

Keywords: Ti-6Al-4V alloy, microstructure, flow softening, finite element analysis

1 Introduction

High-temperature forging and extrusion are widely applied in the aerospace industry. To produce complex shaped structural parts with defect free and homogeneous microstructure, it is essential not only to find optimum processing conditions at high temperature (mechanical aspects), but also to have clear understanding of microstructural evolution during the deformation (microstructural aspects) [1-3]. So far, many investigations have been carried out by use of finite element method (FEM) to predict the distribution of stress, strain and temperature of the deformed parts, but most of the works have ignored the effect of microstructural evolution during the deformation, which often mislead the prediction revealing considerable deviation between experimental results and predicted ones. Therefore, the objectives of this study are to establish more precise constitutive equation based on the compression test data, and to predict the final microstructure with finite element simulation utilizing precise constitutive equation [4].

2 Material and experimental procedures

The material used in the present work was a 95 mm-diameter extruded bar of Ti-6Al-4V supplied from Allegheny technologies. To obtain transformed microstructures (Widmanstätten), as-received material was heat-treated at 1050℃ for 30 min followed by furnace cooling (Fig. 1-(b)).

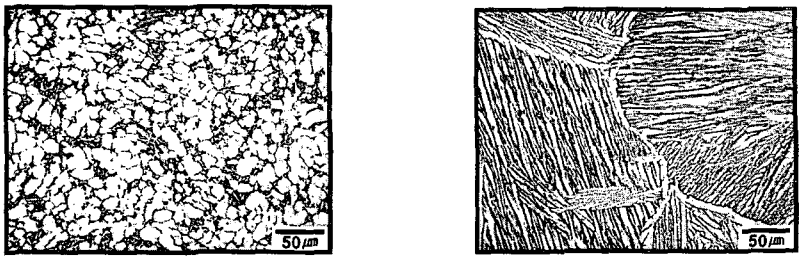

(a) *(b)*

Fig. 1 Two typical microstructures of Ti-6Al-4V alloy used in present study.
(a) equiaxed microstructure and (b) Widmanstätten microstructure (transformed microstructure).

Two microstructures were used as initial microstructures in this study. Equiaxed microstructure consisted of α grains of about 14 μm in diameter with a small amount ($\approx$ 10% in volume fraction) of intergranular β phase. Widmanstätten microstructure revealed several colonies (200 ~ 300 μm) in the prior β grains of about 600 μm in diameter. The width of lamellar α was about 5 μm, and that of grain boundary α layer was 7 μm. Compression test was conducted by use of Gleeble 3500 machine at the temperature range of 700℃ ~ 1100℃ with the strain rate range of 10^{-4} ~ 10^{2}/sec.

3 Results and discussion

The flow stress-strain curves of equiaxed and Widmanstätten microstructures obtained from the compression tests are shown in Fig. 2-(a) and 2-(b), respectively. For both microstructures, deformation was characterized by a peak stress at low strains, flow softening of various degrees, and marked dependence of flow stress on the test temperature. From the curves shown in Fig. 2, various parameters such as strain rate sensitivity (m), activation energy (Q) and etc. were calculated.

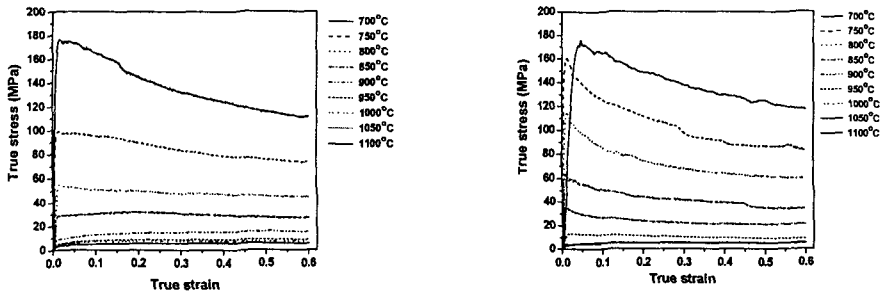

(a) *(b)*

Fig. 2 Flow stress strain-rate curves of Ti-6Al-4V with (a) equiaxed and (b) Widmanstätten microstructures obtained from compression test at various temperatures. The strain rate was constant as 10^{-4}/sec.

Using these parameters, processing maps for two microstructures were evaluated based on the Dynamic Materials Model (DMM) as shown in Fig. 3 [5]. The contour numbers represent the percentage efficiency of power dissipation projected on a temperature-strain rate plane.The processing map for the equiaxed microstructure exhibited two regime of high efficiency. One had a peak efficiency of 60% at 875℃ and 10^{-4}/sec, and the other had a peak efficiency of 45% at 950~1100℃ and 10^{-1}~10^{-2}/sec. These two regions revealing high efficiency of power dissipation are considered as the highly probable regions accompanying microstructural evolution, indicating the best processing conditions without producing any defects in the material. Forming at the low efficiency region (13% at 700℃ and 10^{2}/sec) would produce various defects, which was evidenced by the experiments; cracking along the adiabatic shear band. For the Widmanstätten microstructure, the highest efficiency (65%) occurred at about 975℃ and 10^{-4}/sec.

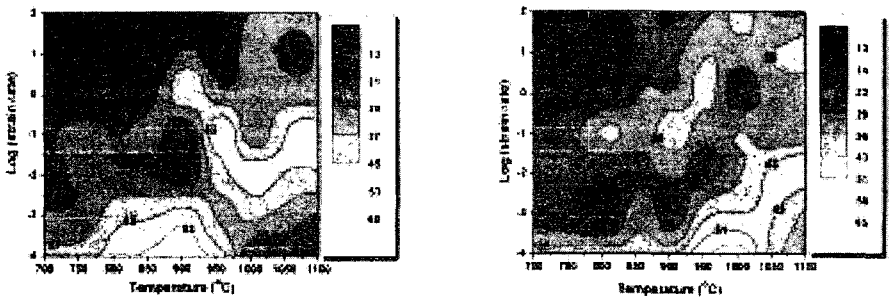

(a) *(b)*

Fig. 3 Processing maps for (a) equiaxed and (b) Widmanstätten microstructure at a strain of 0.6: contour numbers represent a percentage efficiency of power dissipation.

To describe the microstructure evolution during hot working, flow stress-strain curves were analyzed using hyperbolic sine function with internal state variables. Generally, power law (Eq. 1) was most widely used for the simulation and the design processes of metal forming [6].

$$Z = \dot{\varepsilon} \exp\left(\frac{Q}{RT}\right) = A\sigma^{n}; \quad A,\ n: \text{constant} \tag{1}$$

However, the power law shows large deviation with the flow stress data at high stress region, though it shows excellent fit at low stress region [6]. Therefore, the hyperbolic sine function has been used in this study (Eq. 2).

$$Z = \dot{\varepsilon} \exp\left(\frac{Q}{RT}\right) = A\left[\sinh(\alpha\sigma)\right]^{n}; \quad A,\ \alpha, n: \text{constant} \tag{2}$$

By introducing internal state variable, S, Eq. (2) can be extended as following Eq. 3.

$$\dot{\varepsilon}_{ij}^{p} = \frac{3}{2} A \left[\sinh\left(\frac{J_2(\sigma'_{ij}) - k_0}{S}\right)\right]^{n} \exp\left(-\frac{Q}{RT}\right) \frac{\sigma'_{ij}}{J_2(\sigma'_{ij})}, \quad \dot{S} = b^{*}(S_M - S)\varepsilon^{m^{*}}\dot{\varepsilon} \tag{3}$$

Here, k_0 is the initial yield stress in the uniaxial state, b^{*} and m^{*} are two parameters which are dependent on temperature and strain rate. Based on the above mentioned concept, the constitutive equation was developed and FEM was carried out for the backward extrusion process of Ti-6Al-4V alloy. FEM results and optical photographs of actually deformed microstructures were shown in Fig. 4. It is clearly evidenced that measured values of grain size and volume fraction of α phase at different locations of the deformed body are in good agreements with the FEM results.

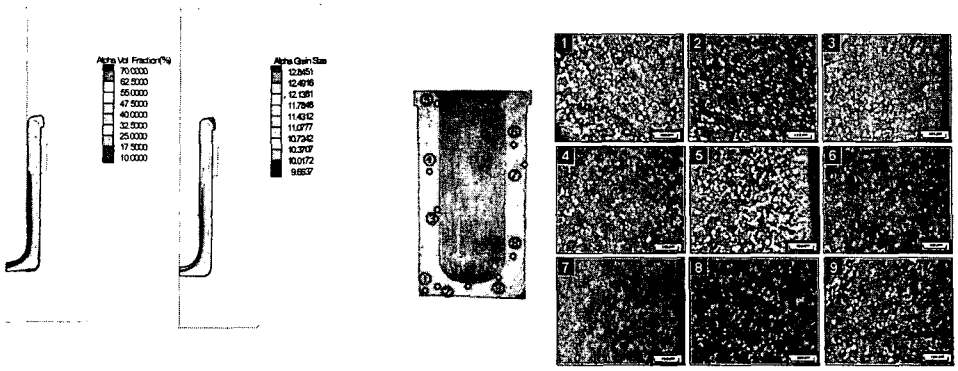

(a) (b) (c)

Fig. 4 FEM simulation results of (a) volume fraction and (b) grain size of α phase, and (c) optical photographs of hot deformed microstructure in backward extruded part.

Table 1 Comparison of measured and simulated grain size and volume fraction of α phase. (Same designation as shown in Fig. 4-(c))

Location		1	2	3	4	5	6	7	8	9
D_α (μm)	measured	10.51	11.76	10.86	11.87	15.97	9.78	13.96	11.18	9.67
	simulated	12.5	13	11.6	12.3	17.4	9	11.6	11.2	9.1
V_α (%)	measured	23.35	18.54	21	20.6	61.43	16.89	57.67	17.3	16.53
	simulated	30.2	22	25	21	64	23.6	49.1	16	22

4 Acknowledgment

This work was financially supported by Agency for Defense Development. The authors are also grateful for the financial support of the 2003 National Research Laboratory Program of the Ministry of Science and Technology of Korea.

5 References

[1] S.L. Semiatin;V. Seetharaman;I. Weiss: Mater. Sci. Eng. A243 (1998), pp. 1
[2] J.S. Kim;Y.W. Chang;C.S. Lee: Met. Trans. A Vol. 29A (1998) pp. 217.
[3] J.S. Kim;J.H. Kim;Y.T. Lee;C.G. Park;C.S. Lee: Mater. Sci. Emg. A263 (1999) pp. 272
[4] W. Bang;C.S. Lee;Y.W. Chang: J. Mater. Proc. Tech. Vol. 134 (2003) pp. 153
[5] Y.V.R.K. Prasad;H.L. Gegel;S.M. Doraivelu;J.C. Malas;J.T. Morgan;K.A. Lark;D.R. Barker: Metall. Trans. A Vol. 15A, October (1984), pp. 1883
[6] M. Zhou;M.P. Clode: Mechanics of Materials 27 (1998), pp. 63